

Effect of Water Saturation on Stability of a Hill Slope: Malin Case Study

Prashant Sudani¹ and Kailas Patil¹

¹ College of Engineering Pune, Geotechnical Engineering, Civil Department, Shivajinagar, 411005, Pune, India

Corresponding author:

Prashant Sudani
sudaniprashant93@gmail.com

Received:
February 26, 2023

Accepted:
April 18, 2023

Published:
June 16, 2023

Citation:

Sudani, P.; and Patil, K. (2023).
Effect of Water Saturation on
Stability of a Hill Slope: Malin Case
Study. *Advances in Civil and
Architectural Engineering*.
Vol. 14, Issue No. 26. pp.138-154
<https://doi.org/10.13167/2023.26.9>

**ADVANCES IN CIVIL AND
ARCHITECTURAL ENGINEERING
(ISSN 2975-3848)**

Faculty of Civil Engineering and
Architecture Osijek
Josip Juraj Strossmayer University
of Osijek
Vladimira Preloga 3
31000 Osijek
CROATIA



Abstract:

The study presents a meticulous investigation into the catastrophic landslide that impacted Malin village in Pune district of Maharashtra, India. By employing a multi-faceted approach encompassing field, laboratory, and numerical analyses, in the study, stability governing parameters were thoroughly assessed with respect to varying levels of water saturation. Field investigation provided crucial insights into the geographical profile, field density, slope strata, and representative soil sample acquired from hill slopes. Furthermore, extensive laboratory investigations were conducted to gain a comprehensive understanding of the role of stability governing parameters under different water saturation levels. The limit equilibrium method was employed for numerical simulation to rigorously evaluate slope stability. The results revealed the significant influence of increased water saturation on stability governing parameters, leading to slope instability, which was confirmed by numerical simulation. The study further established that excessive rainfall triggered the landslide, saturating the soil mass and deteriorating the stability governing parameters, ultimately leading to instability. The findings of this study offer valuable insights for mitigating landslides and can be instrumental in developing effective monitoring and warning systems.

Keywords:

landslide; saturation; stability; geo-hazard

1 Introduction

A landslide is a geological phenomenon that occurs when shear stress acting on a portion of a soil slope surpasses the shear strength of the sliding surface. This landslide event can be triggered by various causative factors, including a steep slope angle, excavation at the toe of the slope, and saturation of the soil slope due to infiltration by rainwater. This is a mass movement of the earth in the downward and outward direction under the influence of gravity. The mass of the earth consists of various soil types, including natural rock, composite soil, and their combinations. The movement of the slide also ranges from a few centimetres to several thousand meters. Three principal types of mass movement are often observed in landslides: falling, sliding, and flowing [1]. A landslide is a catastrophic natural disaster that can create a deep groove in society as it can damage human lives and property. It is triggered by many factors including earthquakes, rainfall [2, 3], and a weak earth layer [4]. Rainfall-induced landslides are the most frequent triggering factors, with several cases reported worldwide [5-7]. India faces many landslides, particularly in the monsoon season, which pose a significant threat to living beings, causing an annual economic loss of 400 million USD [8].

Rainfall has been mainly reported as a landslide-triggering event in Indian landslide research [8-14]. Primarily rainfall infiltrates into the land slope and builds water saturation. Immediately before the monsoon, the slope would be in a dry state. In the dry slope state, capillary suction is present, providing suction strength to the soil mass and improving the shear resistance of the slope. During rainfall, water infiltrates the soil slope and fills capillary pores, thereby reducing soil suction. If more water infiltrates the soil slope, it creates a positive pore water pressure, adversely affecting the stability of the slope [15].

Numerous studies have investigated the occurrence of mass movements and debris flows triggered by rainfall, utilising various theoretical [16, 17], numerical [18-26], experimental, and observational approaches [27, 28]. Many studies focused on laboratory-based experiments to enhance understanding of landslide mechanisms under controlled precipitation conditions. Furthermore, statistical regression analysis has been applied to assess potential slope instability via displacement and pore-water pressure monitoring [8, 11, 29]. Additionally, theoretical frameworks have been proposed to characterise the rainfall hydrology on slopes [30].

A critical aspect that has been overlooked in previous studies is the effect of saturation variation on the stability governing soil parameters such as shear strength, soil suction, and pore water pressure. This study aims to fill this gap by incorporating the effect of saturation variation on stability governing parameters. Additionally, the influence of saturation on the failure mechanism of soil slopes was investigated through limit equilibrium-based numerical simulations to understand the stability status of the slope under varying water saturation levels. This innovative approach aims to provide a more comprehensive understanding of how saturation impacts the stability of soil slopes, thereby contributing to the advancement of landslide research. This research builds upon previous studies that explored changes in subsurface behaviour during landslides and extends the analysis to include the effects of saturation variation on stability parameters. The findings of this study have the potential to significantly enhance understanding of the complex interplay between saturation, soil properties, and slope stability and may have implications for predicting and mitigating landslides in regions prone to rainfall-triggered mass movements.

This study was conducted at an actual landslide site in Malin village, Pune District, India. In the early morning of July 30, 2014, while residents were asleep, a landslide occurred at the study location, "Malin hill slope". This catastrophic event, triggered by prolonged torrential rainfall, obliterated the entire village under the massive flow of soil debris. The scale of the event is presented in Figure 1. The total area affected by the landslide was approximately 44239 m² with a slide depth of 7 m. These mass movement incidents in the western part of the country have resulted in more than hundred deaths, and many casualties [31]. A natural event triggered disastrous failure, and heavy rainfall precipitated continuously in the affected area over the last few days. This resulted in heavy rain saturating the village slope [12].



Figure 1. Impression of landslide event at Malin hill slope [32]

The development of water saturation on the land slope due to prolonged heavy rainfall in the region was the primary triggering factor for the failure of the Malin Hill slope. An investigation of the effects of water saturation on the stability status of the land slope can facilitate an understanding of the effectiveness of saturation monitoring in landslide early warning systems. In this study, a retrospective analysis of the Malin Hill slope was conducted to examine the variation in stability in relation to changes in water saturation. Stability evaluation was performed using limit equilibrium analysis based on Geostudio software. Various saturation levels were analysed, and the effect of these variations on the stability of the land slope was investigated.

1.1 Study area

This study was conducted on the hill slope in Malin Village, situated within the Sahyadri Mountain Range of the Western Ghats, India, particularly in Pune district of Maharashtra. The geographical coordinates of the study location range from 73°40' N to 73°45' N and 19°10' E to 19°5' E. The average height of the surrounding terrain from the mean sea level was 850 m. The average rainfall in the region is approximately 1133,73 mm, and the average temperature of the study location is in the range 20-28 °C [33].

Figure 2 shows a map of the study location, the Malin village hill slope. The surrounding terrain features steep slopes. The topography of Malin village is characterized by highly dissected terrain with flat summits and entrenched valleys. The area is covered by Deccan basalt with the top portion (10 m) of weathered soil. During the monsoon season, the study location typically experiences prolonged rainfall in July and August. It often receives consistent, low-intensity rainfall for extended periods, lasting more than a week, a phenomenon locally termed as “Heli”. This type of prolonged rainfall in locations with steep hill slopes, such as the study area, poses a severe threat of landslide occurrences.

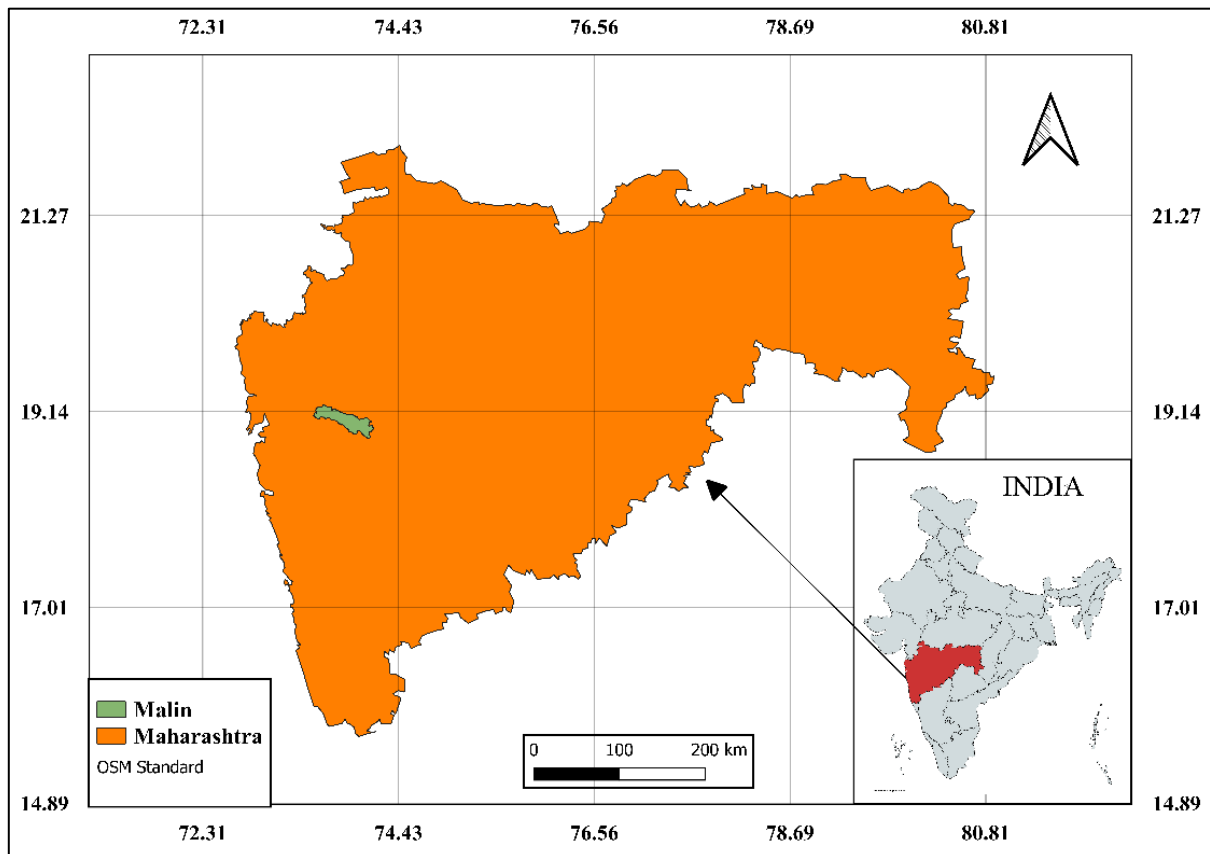


Figure 2. Geographical location of Malin Village

2 Experimental testing: sampling and procedure

The soil sample required for the laboratory investigation was procured during the field investigation. Soil samples were collected from various depths from the surface to stratify the land mass. During the field investigation, the field density of the soil slope was determined by performing a field density test at three different locations using a procedure covered in standard IS 2720 [34]. Dry density was found to be in range of 1,34 to 1,36 g/cc. Field investigations revealed the geographical profile, field density, slope strata, and required representative soil samples. Extensive laboratory investigations revealed the role of stability-governing parameters depending on various water saturations. The slope stability was investigated using the limit equilibrium method via a numerical simulation. The soil required for the study was procured from the study location and tested for various geotechnical properties in a geotechnical engineering laboratory according to the method described in the IS 2720 code of procedure [35-38].

To investigate the influence of varying saturation on the governing parameters of soil stability, a series of soil samples is tested for shear strength at different water saturation levels, as presented. Saturation refers to the percentage of voids in the soil that are filled with water, ranging from 0 %, for unsaturated soil with no water in its voids, to 100 % for fully saturated soil with all voids completely filled with water. Partial saturation represents soil samples with saturation levels between 0 % and 100 %. The motivation for selecting this specific range was to comprehensively encompass the impact of water saturation across the entire spectrum of saturation levels. In every sample simulation for the desired saturation, compaction was limited to achieve a field density. Simultaneously, the effect of saturation on the shear strength of the soil was analysed by performing a shear test. The corresponding changes in the stress–strain profile of the soil with varying saturation were also examined, and critical observations are discussed. The shear test device used in study is shown in Figure 3.

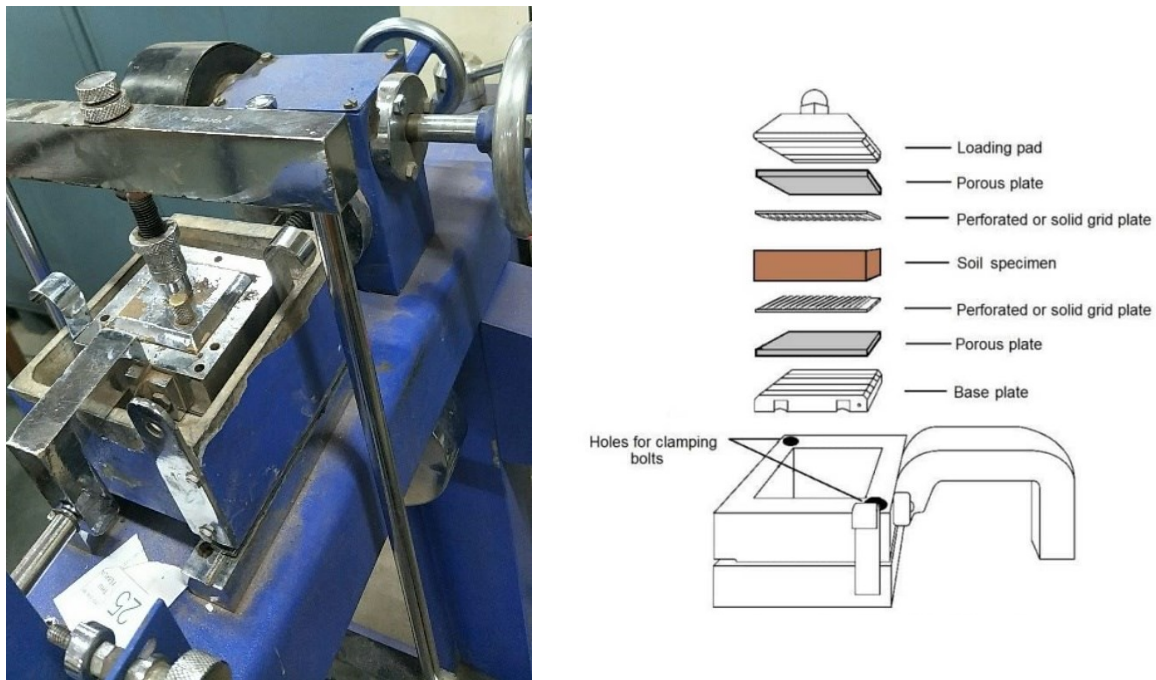


Figure 3. a) Shear test device used in the study; and b) shear box assembly [39]

The soil water characteristic curve (SWCC) was derived by performing filter paper test, following the procedure outlined in ASTM D 5298-03 to determine the effect of saturation on soil matric suction [40]. Further effects on the stability status of hill slopes were performed via limit equilibrium analysis using numerical simulation on Geostudio software, and critical observations were analysed.

2.1 Shear Test

The direct shear test is one of the most useful shear tests for landslide studies owing to its suitability for thin specimens and the apparent analogy of the shearing mechanism to a landslide along a bedding plane [41]. Therefore, a direct shear test was used to assess the soil shear parameters. Furthermore, there are conflicting views regarding the utilisation of a drain or undrained test for assessing the shear parameters. Stark et al. [42] suggested that drained or undrained shear strength may be applicable for materials based on the hydraulic conductivity and loading rate of the material. However, based on the loading rate, [43] noted that an unconsolidated undrained test is preferred when studying the immediate impact of rainwater stored in a slope. This comprehensive evaluation led to the selection of the undrained box shear test for assessing soil shear parameters was deemed appropriate, considering the various factors that influence soil behaviour in landslide-prone areas.

The shear test methodology used in this study adhered to the guidelines provided by the Indian Standard for shear test, specifically IS 2720 Part 13 [43]. Initially, soil samples collected from the field were pulverized and air-dried overnight before testing. The sample size used in the shear box was 90 cm³, with the soil carefully weighed to match the field density identified under field conditions. The soil was compacted in a shear box with limited compaction to achieve the desired density.

The shear test equipment used in this study was a strain-controlled direct shear machine, which included a shear box, soil container, loading unit, proving ring, and dial gauge for measuring shear deformation and shear force. A two-piece square shear box served as the soil container, and a proving ring was used to measure the shear load experienced by the soil along the shearing plane. A constant shear strain rate of 0,125 mm/min was used.

The shear tests conducted in this study applied different normal stresses of 50, 100, and 200 kPa to the soil samples. Soil sample was tested three times at each normal stress level. The relationship between normal stress and shear stress at failure was analysed to determine the soil's failure envelope and to identify the shear strength parameters, specifically cohesion and internal friction angle. The values of 50, 100, and 200 kPa were chosen because they are sufficiently sensitive to measure the shear strength of most soil types, including cohesive and non-cohesive soils. For instance, 50 kPa may be relevant for shallow-foundation designs, while 200 kPa may be more appropriate for deep-foundation designs. Having a range of normal stress values enables the evaluation of soil shear strength under different stress conditions.

2.2 Discussion and results

Field investigations were conducted to explore the Malin Hill slope and to collect the required information and representative soil samples. To understand the stability mechanism of the hill slope, the required geotechnical properties of the soil, such as specific gravity, cohesion, friction angle, soil classification, swelling behaviour, and permeability (Table 1), were determined by laboratory investigations.

Table 1. Geotechnical investigation of soil and observed results based on IS 2720 [44]

S.No.	Description	Unit	Malin soil observed values
1	Natural water content	%	8,60
2	Specific gravity	-	2,70
3	Liquid limit	%	41,00
4	Plastic limit	%	29,66
5	Plasticity index	%	11,34
6	Classification	-	MI – Silt of intermediate plasticity
7	Hydrometer	%	5,85 / 66,15 / 28 Clay/Silt/Sand
8	Free swell	%	23,07
9	Optimum moisture content (OMC)	%	21,00
10	Maximum dry density (MDD)	gm/cc	1,64
11	Cohesion	kPa	69,43
12	Angle of internal friction	°	33,88
13	Permeability	cm/sec	$5,74 \times 10^{-6}$

The geotechnical profile of the slope, along with the locations where the soil samples are collected for laboratory investigations, is presented in Figure 4.

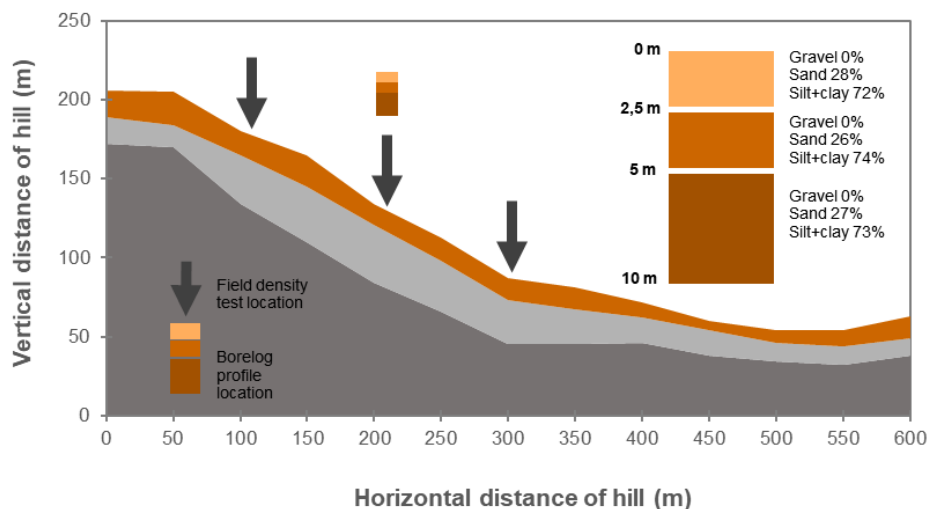


Figure 4. Geotechnical profile of the slope with locations where soil samples were collected

Disturbed soil samples were carefully obtained from designated locations in the laboratory. They were adequately remoulded to replicate field conditions by maintaining the same density. The results are presented as average values of three replicate soil samples.

The field density of the Malin hill slope was 1,365 gm/cc. Based on field density and specific gravity, 34,81 % water content was required to achieve a 100 % saturation for the Malin village hill slope soil. The variation in the water content, represented in increments of 5 %, corresponding to the degree of saturation for soil, is presented in Table 2. This was determined based on the relationship between the specific gravity, void ratio, water content, and dry density of the soil sample, as presented in Equations 1 and 2, for each incremental degree of saturation, the corresponding shear strength parameter cohesion and angle of internal friction of the soil were determined as follows:

$$\gamma_d = \frac{G \cdot \gamma_w}{1 + e} \quad (1)$$

$$e = \frac{W \cdot G}{S_r} \quad (2)$$

Where:

γ_d = dry density of soil (gm/cc),

G = specific gravity of soil,

γ_w = unit weight of water (gm/cc),

e = void ratio of soil,

W = percentage of water content in soil (%), and

S_r = degree of saturation of soil (%).

Table 2. Variation in saturation with respect to change in water content

S.No.	Malin hill slope soil properties		Cohesion (kPa)	Angle of internal friction (°)
	W (%)	S _r (%)		
1	0	0,00	62,68	37,33
2	5	14,36	66,12	35,32
3	10	28,72	69,45	33,88
4	15	43,08	72,20	31,61
5	20	57,44	74,00	27,31
6	25	71,80	60,00	22,65
7	30	86,16	49,05	9,04
8	35	100,00	12,74	4,18

The geological stratification of the soil layers on the bedrock of the Malin Hill slope was investigated. The soil properties were determined in a geotechnical laboratory at the College of Engineering, Pune, under fully saturated conditions. Detailed results are presented and compared in Table 3.

To examine the impact of saturation variation on the shear parameters of the soil from the Malin village hill slope, a series of shear tests were conducted on soil samples with varying degrees of saturation, as depicted in Figure 5. The results underscored the effect of water saturation on two critical parameters governing slope stability, namely cohesion and the angle of internal friction. The finding revealed that cohesion initially experienced a slight increase before substantially decreasing as the degree of saturation rose. This trend can be attributed to the influence of water content on soil consistency. The angle of internal friction exhibited a reduction of up to 4°, signalling an increased risk to slope stability. Specifically, the angle of internal friction decreased from 37,33° to 4,18° with the rise in saturation from 0 % to 100 %

Table 3. Summary of exploration soil data of Malin village hill slope

	Sample	1	2	3
Description	Depth (m)	0,0	2,5	5,0
	To	2,5	5,0	10,0
	Visual description of soil and stratum	Clay silt with relatively intermediate plasticity		
	Hatching			
	IS classification	MI	MI	MI
Particle size analysis	Gravel (%): $\geq 4,75$ mm	0	0	0
	Sand (%): 0,075 to 4,75 mm	28	26	27
	Silt (%): 0,002 to 0,075mm	72	74	73
	Clay (%): $< 0,002$ mm	0	0	0
Atterberg's limit	Liquid limit (%)	41	42	41
	Plastic limit (%)	29,66	30,32	29,44
	Plasticity index (%)	11,30	11,70	11,60
Soil properties	Dry density (gm/cc)	1,35	1,35	1,35
	Natural moisture W (%)	11,50	12,00	11,20
	Specific gravity G_s	2,70	2,70	2,70
	Cohesion (kPa) at 100% saturation	12,74	11,76	12,74
	Friction angle ($^\circ$) at 100% saturation	4,06	4,52	4,26

The cohesion value also decreased from 62,76 kPa at 0 % saturation to 12,74 kPa at 100 % saturation, indicating a substantial decline in these crucial parameters for evaluating soil slope stability. As the soil's moisture content increases, the soil softens due to changes in the distribution of water among soil particles. This results in a decrease in shear strength, cohesion, and the angle of internal friction. When the soil is relatively dry, sliding friction and occlusal friction primarily govern soil behaviour. At low moisture content, the shear strength was higher because of the increased sliding friction between the soil particles and matric suction. However, as the moisture content increased, the suction force declined, leading to a greater distance between soil particles, a weakened cementing force, and a reduced friction coefficient during shear testing.

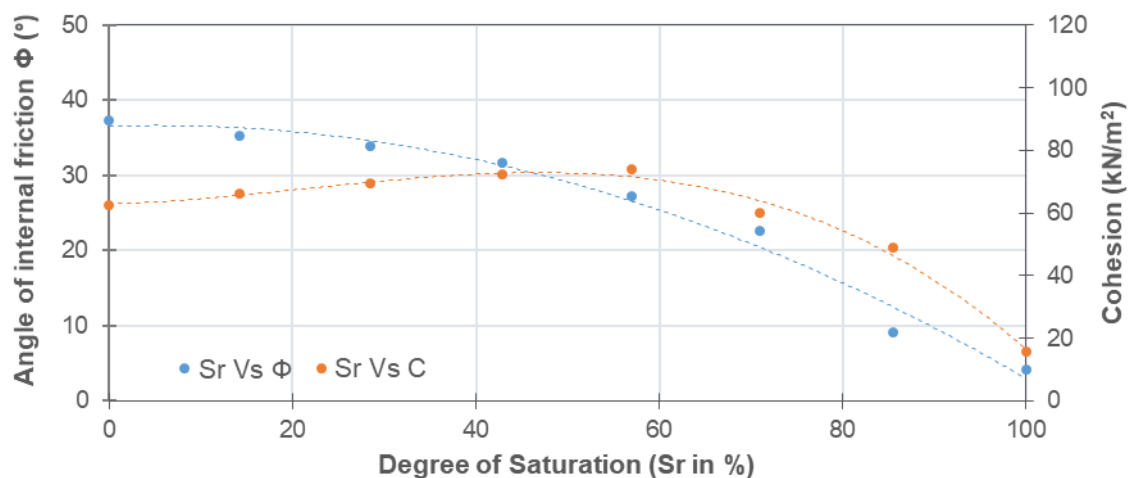


Figure 5. Effect of saturation variation on the stability governing parameters, i.e., cohesion and the angle of internal friction

The stress–strain profiles of the Malin hill slope soil, as presented in Figure 6, show that in the early phase, when the degree of saturation is low, the curve exhibits a peak and then fails, indicating the brittle plastic failure of the soil. However, as the degree of saturation increases, the stress–strain curves tend to flatten toward the X-axis, representing the plastic type of soil failure. This may be due to the higher water content of the soil sample, which makes the soil very soft and flowable. In this context, it can be observed that with an increase in the degree of saturation, the failure mode transforms from brittle–plastic to plastic. With an increase in the degree of saturation, the strain at failure increased, indicating that a large strain is required at a higher saturation to cause slope failure.

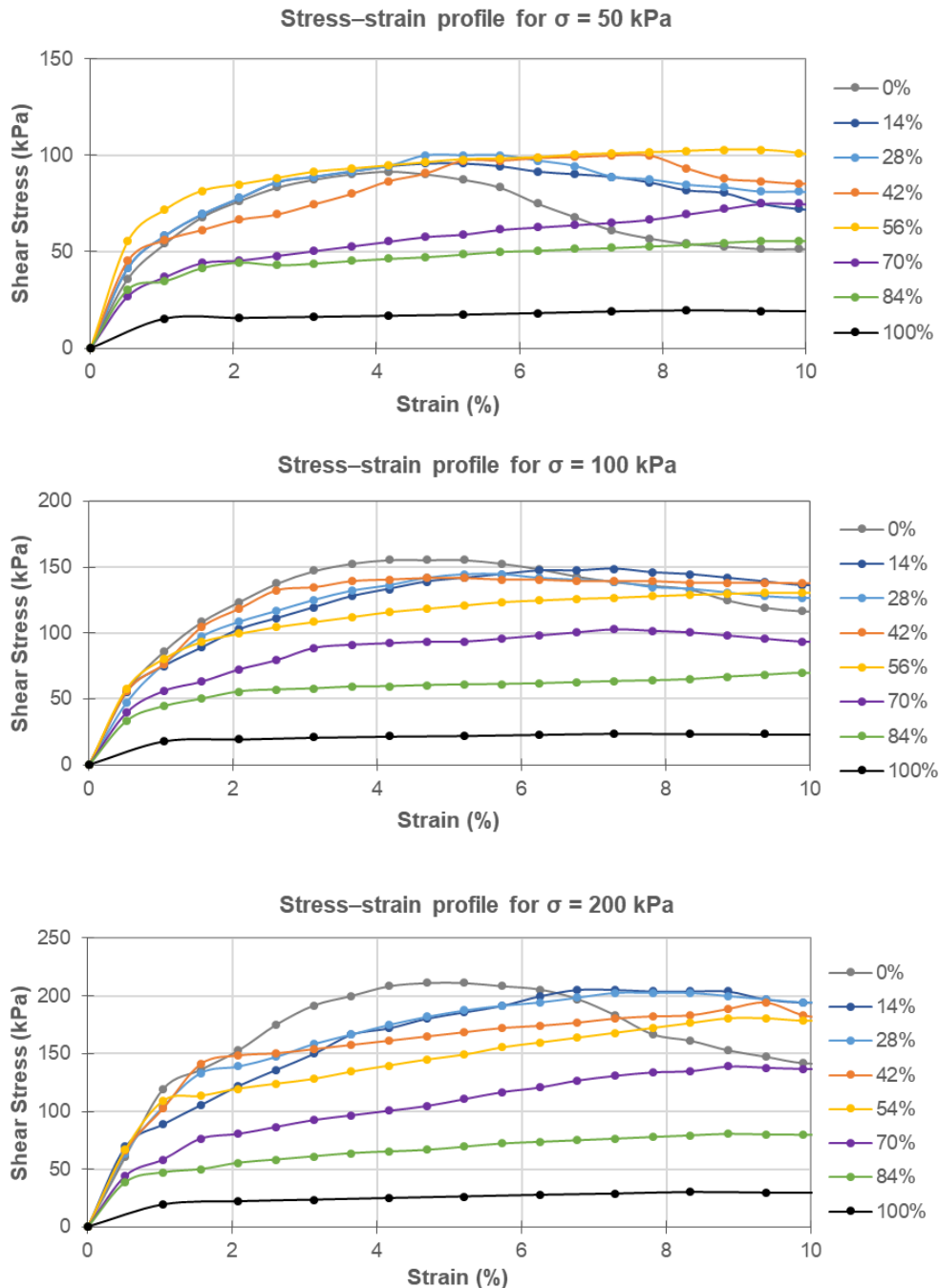


Figure 6. Stress–strain profiles of the Malin hill slope soil with respect to different normal stress values

Figure 7 shows the saturation effect on the maximum stress and the corresponding strain rate for all three normal stresses of 50 kPa, 100 kPa, and 200 kPa. The graph shows that if the degree of saturation increases, the maximum shear stress corresponding to the same normal stress decreases, and the corresponding strain rates increase.

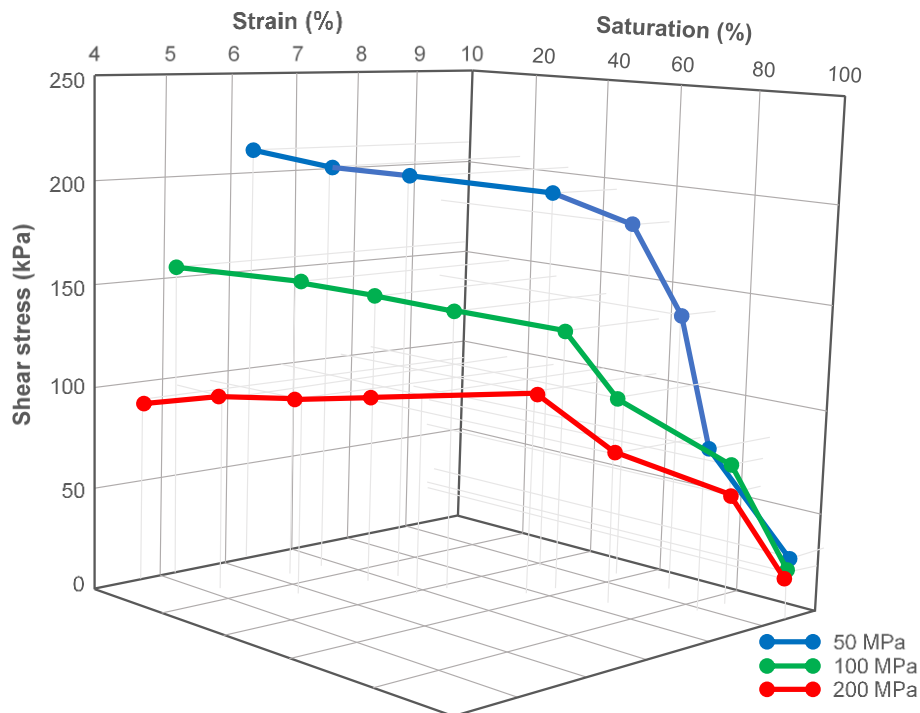


Figure 7. Effect of saturation on the maximum stress and their corresponding strain rate

It is determined that, with an increasing degree of saturation, maximum strain at failure corresponding to the same normal stress increases to 100,00 %, 80,76 %, and 77,60 % for normal stress of 50, 100, and 200 kPa, respectively. Furthermore, it was observed that with an increasing degree of saturation, maximum shear stress corresponding to the same normal stress decreased up to 77,80 %, 85.1 %, and 85.64 % for normal stresses of 50, 100, and 200 kPa respectively. This might be due to the increasing softening of the soil, which makes the soil more flowable or has low strength. This increase in soil fluidity was the reason for the higher strain rate at failure with a higher degree of saturation. The failure strain increased with an increase in the normal stress of the soil. This is because the soil was compacted according to the stress applied at a higher normal stress and required more strain to reach failure.

2.3 Effect of saturation on matric suction and piezometric head

In the dry state, soil suction (negative pore water pressure) reaches its maximum. Conversely, when the soil is fully saturated ($S_r = 100\%$), the positive pore pressure reaches its peak. Between these two extremes, the soil achieves zero water pressure at a certain point. The field capacity, representing the volumetric water content at which the soil reaches zero pore water pressure, is a critical parameter [45]. The field capacity of the soil from the Malin village slope was determined by preparing a soil sample in a cylindrical barrel at field density and moisture content. Additional water was incrementally added to the top of the barrel until water began to seep from the bottom outlet. Once water started collecting at the bottom, the capillary porosity was deemed fully saturated, and the matric suction reached zero. Any further accumulation of water in the system creates a positive pore water pressure in the soil.

Figure 8 illustrates the accumulation of water in the top 10 m of the weathered soil on the Malin village hill slope. Initially, the soil was dry ($S_r = 0\%$) with a porosity (n) of 0,47. Up to a

volumetric water content (VWC) of 34 %, water accumulated and was retained in the capillary pores. The effective porosity, which is the difference between the total porosity and field capacity (where the soil reaches zero matric suction), is a key metric. In this case, the effective porosity (n_{eff}) is 0,13 (i.e., $0,47-0,34 = 0,13$). This indicates that once zero pore water pressure is attained, a positive change in volumetric water content of 13 % would lead the piezometric line to 10 m (Figure 5). The volumetric water content θ will vary between a maximum value θ_{max} and a minimum value θ_{min} . Excess water, where $\theta > \theta_{max}$, may temporarily be stored, generating positive pore water pressure in the soil, and later removed from the system through percolation.

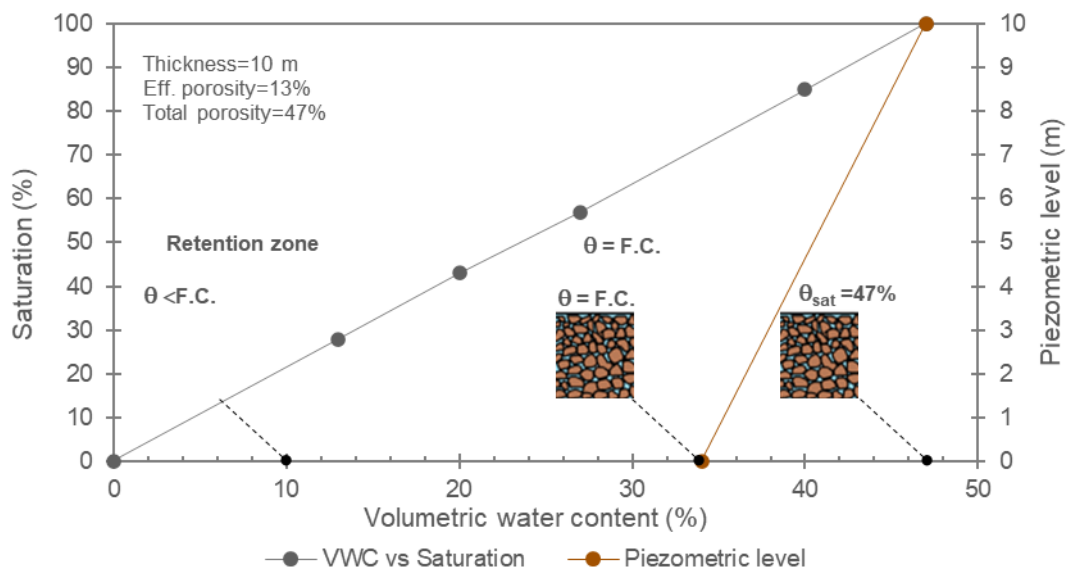


Figure 8. Volumetric water content, saturation, and piezometric relationship for Malin soil

To investigate the effect of water saturation on the shear behaviour during its unsaturated state, the soil water characteristic curve (SWCC) was derived as per the procedure given by ASTM D-5298-16 [40], which provides a standard test method for measuring soil suction using filter paper (Figure 9).

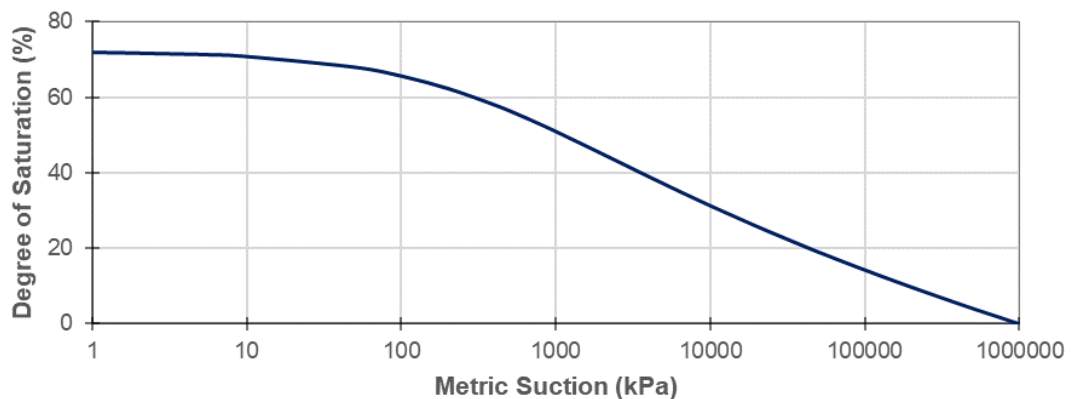


Figure 9. Soil water characteristic curve (SWCC) of Malin hill slope soil

SWCC can be used to determine soil shear behaviour within the range of degrees of saturation from 0 to 72 %. At 72 % of water saturation, suction is found to be zero. Further addition of water into the soil system results in a positive pore water pressure, as shown in Figure 5.

2.4 Effect of saturation on stability of hill slope

The stability status of the land slope was evaluated using the limit equilibrium method (LEM) with the aid of GeoStudio software. The SEEP/W and SLOPE/W modules from GeoStudio were utilized to examine the stability of the slope. The stability analysis employed the Morgenstern and Price's method with a half-sine function. To effectively account for interslice forces, satisfying both the force and moment equilibria. Incorporating interslice forces into the stability analysis enhances the accuracy of the results.; a more simplified method that excludes interslice forces and does not satisfy all equilibrium equations can sometimes lead to unsafe conclusions. The Morgenstern–Price method considers both shear and normal interslice forces, fulfils both force and moment equilibria conditions, and enables a range of user-selected interslice force functions.

A slope stability analysis is conducted on the actual geometry of the Malin village hill slope, as depicted in Figure 10. The slope measures 205 m in height and 1200 m in width at the base, with varying natural slope angles across its surface. The slope is composed of three layers: i) a top layer of weathered soil; ii) second layer of massive basalt rock; and iii) third layer of vesicular basalt rock. The geotechnical parameters of the geomaterials that form the hill slope are presented in Table 4.

Table 4. Geotechnical parameters of the geomaterials that form the hill slope

Soil/rock	Dry unit weight (kN/m ³)	Cohesion (kPa)	Friction angle (°)
Soil (top layer) (at 100 % S _r)	13,34	12,74	4,18
Massive basalt (middle layer)	28,50	910,50	39,40
Vesicular basalt (bed layer)	25,50	810,10	38,00

The slope analysis results revealed the effect of water saturation on the stability of the hill slope. The results presented in Figure 11 show that as the saturation builds in the slope's soil mass, its stability degrades. Initially, the 0% water saturation case simulated the dry state of the slope, which can represent the slope during the summer season.

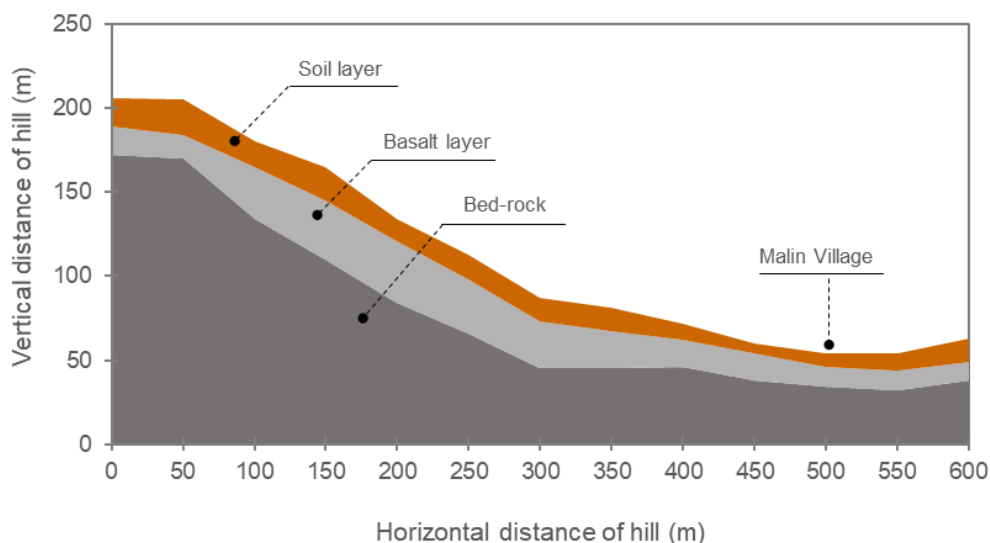


Figure 10. Geometry of Malin village hill slope

Other cases simulated various slope conditions that varied during the monsoon and winter seasons. During monsoons, owing to rainfall infiltration and percolation, this saturation value varies continuously and must be monitored to develop an efficient landslide early warning system. The compiled output of the stability analysis is shown in Figure 8.

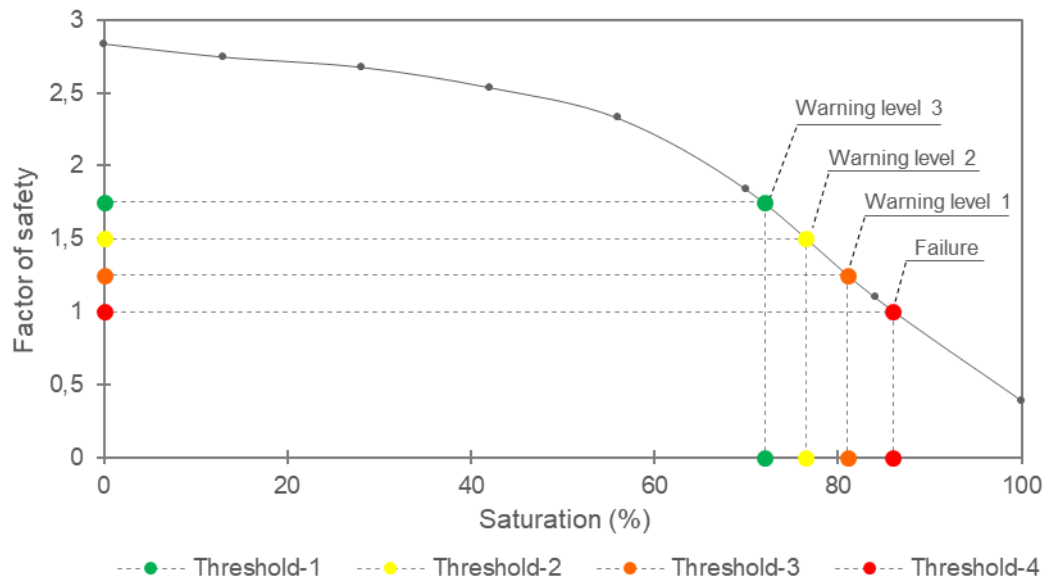


Figure 11. Effect of water saturation on the stability status of the Malin hill slope along with defined warning levels

The research shows that the effect of variation in the water saturation in the soil mass up to 60 % on the slope stability is insignificant. The slope was stable during this variation, with a minimum safety factor of 2,25 (Figure 11). Beyond 60 % water saturation, slope stability was found to decrease drastically, and the reported safety factor was 1 at 87 % degree of water saturation. This can be due to the higher percentage of water content in the soil mass, which is responsible for the loss of soil suction strength and increase in soil pore water pressure. After reaching 60 % water saturation, a further 27 % increase in saturation causes the factor of safety to decrease from 2,25 to 1, indicating potential slope failure. This 27 % variation, specifically from 60 % to 87 % saturation, is crucial.

3 Conclusions

This study examines the impact of water saturation on stability-governing parameters and its subsequent effect on land slope stability, using real-life landslide examples as case studies. The following conclusions were drawn based on a thorough analysis:

- When considering cohesion and the angle of friction, it was found that as water saturation increased in the soil, cohesion initially experienced a slight increase before decreasing. The angle of friction was found to lose its value by up to 70 %.
- In terms of the soil's stress–strain behaviour, an increase in the degree of saturation led to a transformation in the failure mode from brittle-plastic to plastic. It was also observed that with an increase in the degree of saturation, the strain at failure rose, indicating that higher strain is required for soil failure at increased saturation levels.
- When studying the impact of saturation on suction and piezometric head, it was found that suction strength decreases to zero once the volumetric water content reaches up to 34 %. Any positive variation in VWC beyond this point led to an increase in the piezometric head in the soil.

- A numerical investigation of slope stability demonstrated the impact of water saturation on landmass stability. The analysis revealed that variations in water saturation within the soil mass, up to 60 %, did not significantly impact slope stability. The slope remained stable during this variation, with a minimum safety factor of 2,25. However, beyond 60 % water saturation, slope stability was found to drop drastically, with the reported safety factor reaching 1 at 87 % water saturation. This can be attributed to the high percentage of water content in the soil mass, which leads to a loss of soil strength and increased soil flowability. After 60% water saturation, a 27% increase in saturation caused the safety factor to drop from 2,25 to 1, indicating potential slope failure. This 27 % saturation variation, particularly from 60 % to 87 % of saturation, is critical.

This paper presents a site-specific approach to analysing land slope stability, which can serve as a powerful tool for monitoring and warning systems. Before applying the methodology described in this study for monitoring and warning purposes in other locations, it is essential to conduct comprehensive testing and analysis. In addition, its practicality and effectiveness, the proposed approach able to provides saturation-based warning levels that can be monitored in real time.

Acknowledgments

The authors are grateful to the AICTE doctoral fellowship (ADF) scheme for providing a research fellowship for the PhD course. Furthermore, the authors extend their gratitude to the College of Engineering, Pune, for providing research facilities.

References

- [1] Varnes, D. J. Landslide types and processes. In: *Landslides and Engineering Practice*, Eckel, E. B. (ed.). Washington D.C., USA: Highway Research Board; 1958.
- [2] Rahardjo, H.; Lee, T. T.; Leong, E. C.; Rezaur, R. B. Response of a residual soil slope to rainfall. *Canadian Geotechnical Journal*, 2005, 42 (2), pp. 340-351. <https://doi.org/10.1139/t04-101>
- [3] Collins, B. D.; Znidarcic, D. Stability Analyses of Rainfall Induced Landslides. *Journal of Geotechnical and Geoenvironmental Engineering*, 2004, 130 (4), pp. 362-372. [https://doi.org/10.1061/\(ASCE\)1090-0241\(2004\)130:4\(362\)](https://doi.org/10.1061/(ASCE)1090-0241(2004)130:4(362))
- [4] Hsu, S.-C.; Nelson, P. P. Material spatial variability and slope stability for weak rock masses. *Journal of Geotechnical and Geoenvironmental Engineering*, 2006, 132 (2), pp. 183-193. [https://doi.org/10.1061/\(ASCE\)1090-0241\(2006\)132:2\(183\)](https://doi.org/10.1061/(ASCE)1090-0241(2006)132:2(183))
- [5] Di Carluccio, G.; Pinyol, N. M.; Alonso, E. E.; Hürlimann, M. Liquefaction-induced flow-like landslides: the case of Valarties (Spain). *Géotechnique*, 2023, pp. 1-18. <https://doi.org/10.1680/jgeot.21.00112>
- [6] Sudani, P.; Patil, K. A. Evolution of Early Warning System for Landslides. *Disaster Advances*, 2022, 15 (8), pp. 46-59. <https://doi.org/10.25303/1508da046059>
- [7] Wicki, A. et al. P. Assessing the potential of soil moisture measurements for regional landslide early warning. *Landslides*, 2020, 17 (8), pp. 1881-1896. <https://doi.org/10.1007/s10346-020-01400-y>
- [8] Ramesh, M. V. Design, development, and deployment of a wireless sensor network for detection of landslides. *Ad Hoc Networks*, 2014, 13 (A), pp. 2-18. <https://doi.org/10.1016/j.adhoc.2012.09.002>
- [9] Kunnath, A. T.; Ramesh, M. V. Integrating Geophone Network to Real-Time Wireless Sensor Network System for Landslide Detection. In: *The First International Conference on Sensor Device Technologies and Applications*, Yurish, S.; Yufera, A.; Ferrari, V.; Popescu, M. (eds.). 18-25 July 2010, Venice, Italy, IEEE Computer Society, Conference Publishing Services (CPS); 2010, pp. 167-171. <https://doi.org/10.1109/SENSORDEVICES.2010.38>

- [10] Ering, P. et al. Forensic analysis of Malin landslide in India. In: *International Symposium on Geohazards and Geomechanics (ISGG2015)*. 10-11 September 2015, Warwick, UK, IOP Conference Series: Earth and Environmental Science; 2015. <https://doi.org/10.1088/1755-1315/26/1/012040>
- [11] Sardana, S.; Verma, A. K.; Verma, R.; Singh, T. N. Rock slope stability along road cut of Kulikawn to Saikhamakawn of Aizawl, Mizoram, India. *Natural Hazards*, 2019, 99, pp. 753-767. <https://doi.org/10.1007/s11069-019-03772-4>
- [12] Sarvade, S. M.; Sarvade, M. M.; Khadatare, P. S.; Kolekar, M. R. 30/7 malin landslide: a case study. In: *Proceedings of National Conference "GEPSID"*, Singh, H.; Jha, J. N.; Kaur, P.; Sinha, A. (eds.). 11-12 October, 2014, Ludhiana, India, Guru Nanak Dev Engineering College Ludhiana; 2014, pp. 691-698.
- [13] Shah, C. R.; Sathe, S. S.; Bhagawati, P. B.; Mohite, S. S. A hill slope failure analysis: A case study of Malingoan village, Maharashtra, India. *Geology, Ecology, and Landscapes*, 2021, 5 (1), pp. 1-6. <https://doi.org/10.1080/24749508.2019.1695714>
- [14] Sudani, P.; Patil, K. A. Geo-Mechanical Behavior of Toe Excavated Land Slope. *International Journal of Mechanical Engineering*, 2022, 7 (6), pp. 319-327.
- [15] Keefer, D. K. et al. Real-time landslide warning during heavy rainfall. *Science*, 1987, 238 (4829), pp. 921-925. <https://doi.org/10.1126/science.238.4829.921>
- [16] Spross, J. et al. Risk management procedure to understand and interpret the geotechnical context. *Georisk: Assessment and Management of Risk for Engineered Systems and Geohazards*, 2021, 16 (2), pp. 235-250. <https://doi.org/10.1080/17499518.2021.1884883>
- [17] Zhang, J. et al. Performance-based assessment of permanent displacement of soil slopes using two-dimensional dynamic analysis. *Georisk: Assessment and Management of Risk for Engineered Systems and Geohazards*, 2021, 16 (1), pp. 178-195. <https://doi.org/10.1080/17499518.2021.2010765>
- [18] Kumar, S.; Pandey, H. K. Slope Stability Analysis Based on Rock Mass Rating, Geological Strength Index and Kinematic Analysis in Vindhyan Rock Formation. *Journal of the Geological Society of India*, 2021, 97, pp. 145-150. <https://doi.org/10.1007/s12594-021-1645-y>
- [19] Luo, J. et al. Probabilistic model calibration of spatial variability for a physically-based landslide susceptibility model. *Georisk: Assessment and Management of Risk for Engineered Systems and Geohazards*, 2021, 16 (4), pp. 728-745. <https://doi.org/10.1080/17499518.2021.1988986>
- [20] Sudhanvakrishna, G.; Harshith, U. S.; Mohith, Y. S.; Mujeeb, A. Slope Stability Analysis of Hattihole and Kandanakolli Regions Using Geostudio 2018 Slope/W Software. *Institute of Scholars (InSC)*, 2020, pp. 1132-1137.
- [21] Rathore, V.; Sahu, A. K. Slope stability and factor of safety analysis on different region of soil by using geo studio slope/w software. *Journal of Geotechnical Engineering*, 2020, 7 (3). <https://doi.org/10.37591/joge.v7i3.4260>
- [22] Yu, R.; Huang, Z.; Yang, Z. Surface-mining slope reinforcement design based on GeoStudio and FLAC3D. *Mining Science*, 2022, 29, pp. 141-163. <https://doi.org/10.37190/msc222909>
- [23] Gian, Q. A. et al. Design and implementation of site-specific rainfall-induced landslide early warning and monitoring system: a case study at Nam Dan landslide (Vietnam). *Geomatics, Natural Hazards and Risk*, 2017, 8 (2), pp. 1978-1996. <https://doi.org/10.1080/19475705.2017.1401561>
- [24] Chakraborty, R.; Dey, A. Effect of toe cutting on hillslope stability. In: *Lecture Notes in Civil Engineering*, di Prisco, M. et al. (eds.). Singapore: Springer; 2018, pp. 191-198. https://doi.org/10.1007/978-981-13-0368-5_21
- [25] Krahn, J. Stability Modeling with SLOPE/W An Engineering Methodology. Alberta, Canada, GEO-SLOPE International, Ltd.; 2014. Accessed: 14.06.2023. Available at: https://www.u-cursos.cl/ingenieria/2010/1/C144B/1/material_docente/bajar?id_material=297149

- [26] Ganta, N. R.; Satyam, N. Investigation of Failure Mechanism of Lungchok Landslide, Sikkim (India). *Preprints.org*, 2019. <https://doi.org/10.20944/preprints201908.0230.v1>
- [27] Khorasani, E.; Amini, M.; Hossaini, M. F.; Medley, E. Evaluating the effects of the inclinations of rock blocks on the stability of bimrock slopes. *Geomechanics and Engineering*, 2019, 17 (3), pp. 279-285. <https://doi.org/10.12989/gae.2019.17.3.279>
- [28] Supper, R. et al. Geoelectrical monitoring: An innovative method to supplement landslide surveillance and early warning. *Near Surface Geophysics*, 2014 12 (1), pp. 133-150. <https://doi.org/10.3997/1873-0604.2013060>
- [29] Abraham, M. T. et al. Developing a prototype landslide early warning system for Darjeeling Himalayas using SIGMA model and real-time field monitoring. *Geosciences Journal*, 2022, 26, pp. 289-301. <https://doi.org/10.1007/s12303-021-0026-2>
- [30] Lucas, D. et al. Modelling of landslides in a scree slope induced by groundwater and rainfall. *International Journal of Physical Modelling in Geotechnics*, 2020, 20 (4), pp. 177-197. <https://doi.org/10.1680/jphmg.18.00106>
- [31] Ering, P.; Sivakumar Babu, G. L. Probabilistic back analysis of rainfall induced landslide- A case study of Malin landslide, India. *Engineering Geology*, 2016, 208, pp. 154-164. <https://doi.org/10.1016/j.enggeo.2016.05.002>
- [32] Dey, N.; Sengupta, A. Effect of rainfall on the triggering of the devastating slope failure at Malin, India. *Natural Hazards*, 2018, 94, pp. 1391-1413. <https://doi.org/10.1007/s11069-018-3483-9>
- [33] Vilas, P.; Ramesh, G. A geographical study of landslide: A case study of malin village of ambegaon tahsil in pune district, Maharashtra. *Peer Reviewed International Research Journal of Geography*, 2018, 35 (1), pp. 55-60.
- [34] Bureau of Indian Standards. IS:2720 (part XXIX)-1975: Indian Standard Method of Test for Soils: Determination of Dry Density of Soils In-place by the Core-Cutter Method. Accessed: 14.06.2023. Available at: <https://ia803000.us.archive.org/32/items/gov.in.is.2720.29.1975/is.2720.29.1975.pdf>
- [35] Bureau of Indian Standards. IS:2720 (Part-1)-1983: Methods of test for soils, Part 1: Preparation of dry soil samples for various tests. Accessed: 14.06.2023. Available at: <https://law.resource.org/pub/in/bis/S03/is.2720.1.1983.pdf>
- [36] Bureau of Indian Standards. IS:2720 (Part 5)-1985: Determination of Liquid limit and Plastic limit of soil. Accessed: 14.06.2023. Available at: <https://ia600409.us.archive.org/35/items/gov.in.is.2720.5.1985/is.2720.5.1985.pdf>
- [37] Bureau of Indian Standards. IS:2720 (Part 4)-1985: Methods of Test for Soils, Part 4: Grain Size Analysis. Accessed: 14.06.2023. Available at: <https://ia803007.us.archive.org/35/items/gov.in.is.2720.4.1985/is.2720.4.1985.pdf>
- [38] Bureau of Indian Standards. IS:2720 (Part XXII)-1972: Indian Standard Methods of test for soil: Part XXII Determination of Organic Matter. Accessed: 14.06.2023. Available at: <https://www.cracindia.in/admin/uploads/IS-2720---22.pdf>
- [39] Head, K. H.; Epps, R. J. *Manual of soil laboratory testing, vol. II: Permeability, Shear Strength and Compressibility Tests*. 3rd edition, Dunbeath, Caithness, Scotland, UK: Whittles Publishing.
- [40] ASTM D5298-16. Standard Test Method for Measurement of Soil Potential (Suction) Using Filter Paper. November 1994.
- [41] Aramaki, S.; Kitazono, Y.; Suzuki, A.; Kajiwara, M. Application of direct shear test to analysis of tertiary landslides along a bedding plane. *Soils and Foundations*, 1992, 32 (1), pp. 1-12. <https://doi.org/10.3208/sandf1972.32.1>
- [42] Stark, T. D.; Choi, H.; McCone, S. Drained Shear Strength Parameters for Analysis of Landslides. *Journal of Geotechnical and Geoenvironmental Engineering*, 2005, 131 (5), pp. 575-588. [https://doi.org/10.1061/\(ASCE\)1090-0241\(2005\)131:5\(575\)](https://doi.org/10.1061/(ASCE)1090-0241(2005)131:5(575))
- [43] Bureau of Indian Standards. IS:2720 (Part 13)-1986: Methods of test for soils, Part 13: Direct shear test. Accessed: 14.06.2023. Available at: <https://law.resource.org/pub/in/bis/S03/is.2720.13.1986.pdf>

- [44] Bureau of Indian Standards. IS:2720 (Part 17)-1986: Methods of test for soils, Part 17: Laboratory determination of permeability. Accessed: 14.06.2023. Available at: <https://law.resource.org/pub/in/bis/S03/is.2720.17.1986.pdf>
- [45] Fiorillo, F.; Wilson, R. C. Rainfall induced debris flows in pyroclastic deposits, Campania (southern Italy). *Engineering Geology*, 2004, 75 (3-4), pp. 263-289. <https://doi.org/10.1016/j.enggeo.2004.06.014>